Synthesis, Characterization and Biological Studies of Ce and Y-Luteolin Complexes

Nurudeen Gidado[1], Mukhtar Haruna[1], Fartisincha P. Andrew[2] and Musbahu Yahaya[3]

[1]Department of Chemistry, Faculty of Physical Sciences, Modibbo Adama University, Yola, Adamawa State, Nigeria

[2]Department of Science Laboratory Technology, Faculty of Life Sciences, Modibbo Adama University, Yola, Adamawa State, Nigeria

[3]Department of Chemistry, Faculty of Natural and Applied Sciences, Sule Lamido University, Kafin Hausa, Jigawa State, Nigeria

DOI: https://doi.org/10.51244/IJRSI.2026.1310000047

Received: 12 October 2026; Accepted: 17 October 2026; Published: 31 October 2026

ABSTRACT

The rising threat of antimicrobial resistance necessitates novel agents with improved efficacy. The study aimed to synthesized, characterized and evaluate the antimicrobial activities of Ce(III) and Y(III)-Luteolin complexes. The complexes were prepared in 1:3 metal to ligand ratio by refluxing aqueous metal salts with luteolin in ethanolic solution at pH 6.9. The compounds were characterized using FT-IR, solubility test, molar conductivity, magnetic susceptibility and elemental analysis, UV-visible, Thermogravimetric analysis (TGA) and powder X-ray diffraction (XRD. Antimicrobial activity was assessed by agar-well diffusion methods against bacterial strains (*Staphylococcus aureus* and *Escherichia coli*) and fungal strains (*Candida albicans* and *Aspergillus niger*). The complexes showed a percentage yield of 68.82 for Ce and 83.96 for Y-complexes respectively. The ligand and its synthesized complexes were found to be insoluble in water and n-hexane but soluble in DMSO. The ligand melt at 316^0C while the complexes decomposed at 351 for Ce^0C-complex and 357^0C Y-complex suggesting the complexes to be thermally stable than the ligand and cannot decomposed easily. The FT-IR spectra of luteolin showed a broad band at 3198 cm^{-1}, assignable to phenolic (OH). Another sharp absorbance band seen at 1659 cm-1 assigned to aromatic C=O stretch in the ligands were shifted to lower frequency range of 1651 - 1653 cm^{-1}, suggesting coordination through oxygen of the C=O of the ligands respectively. New bands at the lower region in the range of 628 - 623 cm^{-1} which were not observed in the ligand, further confirmed M--O chelation in the complexes, which confirmed the deprotonation of phenolic (OH) in the ligands. The magnetic susceptibility data suggest paramagnetism of Ce-complex and diamagnetism property for Y-complexes. The UV-visible band shifted bathochromically comparted to the ligand. Molar conductivity results indicate the complexes to be non-electrolyte due to lower values obtain (1.55-8.60 $ohm^{-1}cm^{-1}mol^{-1}$). The TGA results revealed sequential loss of lattice and coordinated water. The elemental analysis result showed that there is good agreement between the theoretical and experimental value suggesting the proposed structure was achieved. The XRD pattern confirmed crystalline materials distinct from free luteolin. All complexes exhibited concentration-dependent antimicrobial activities superior to the free luteolin.

Keywords: Cerium. Luteolin, Yttrium, Coordination Chemistry, Antimicrobial Activity.

INTRODUCTION

The field of bioinorganic chemistry has witnessed increasing attention toward the study of metal-organic complexes, particularly those involving bioactive ligands such as flavonoids (Yuanyong Yao 2020). Flavonoids are naturally occurring polyphenolic compounds widely distributed in plants, renowned for their antimicrobial, antioxidants and anticancer activities (Kumar *et al.*, 2021), these molecules are synthesized by plants and can be found abundantly in seeds and fruits, it determines the color, flavor, and other organoleptic

ISSN No. 2321-2705 | DOI: 10.51244/IJRSI |Volume XIII Issue X October 2026

characteristics of the plant. As well as contributing to its nutritional aspects and are considered bioactive compounds. (Sabirna*et al* 2022). Flavonoids are considered secondary metabolites that play protective roles in plants against ultraviolet radiation, microbial attack, and oxidative stress (wenbin*et al.,* 2023). Flavonoids share a common structural motif defined by a C_6-C_3-C_6 carbon framework consisting of two aromatic rings connected by a three-carbon units that commonly forms a heterocyclic C ring. Variations in the oxidation state substitution pattern of this framework give rise to several flavonoids classes including flavones, which encompass compounds such as luteolin and apigenin, flavonols, which include quercetin and kaempferol, flavanones such as naringenin, isoflavones like genistein, anthocyanidins, which contribute to pigmentation in plants, and flavan-3-ols, which are commonly found in tea and chocolate. Each class exhibits distinct chemical characteristics that influence their reactivity, bioavailability, and biological functions. (Vakarelska-Popovska, *et al.,* 2022).

Luteolin is a Yellow crystalline powder has Molecular Weight 286.24 g/mol, Melting Point ranges from 328-330 °C (decomposes), insoluble in water, soluble in ethanol, and methanol. Itsabsorbs UV-Vis in the region of 250-380 nm range. Luteolin is Sensitive to light and moderate thermal stability (Vakarelska, *et al.,* 2022). Luteolin, is one of the flavonoid compounds discovered in celery, rosemary, onions and parsley with a molecular formula $C_{15}H_{10}O_6$ and and belong to class flavones. it contains four hydroxyl groups located at positions 3′, 4′, 5, and 7. This arrangement results in a planar flavone backbone that facilitates π-electron delocalization and enhances the molecule's ability to engage in redox reactions. Its structure includes multiple metal-binding sites, most notably the 5-hydroxy-4-carbonyl moiety, which serves as a primary chelation site, and the 3′,4′-dihydroxy catechol system on ring B, which constitutes a second major metal-binding site. These features contribute to its strong metal-chelating ability (Bonetti F, *et al.*,2017 and Vakarelska, *et al.*,2022).

The complex of $Ce^{3+,}$ and Y^{3+} ions with luteolin will results the formation of stable metal-ligand, enhanced antimicrobial activity when compared to free luteolin. This is based on the coordinating lanthanide ions with the hydroxyl and oxo group of the ligand(Luteolin) will improve the ligand's solubility, stability, and ability to interact with microbial biomolecules.

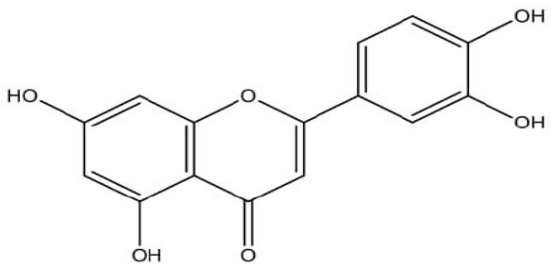


Figure 1: Chemical Structure of Luteolin**3',4',5,7-Tetrahydroxyflavone**

MATERIALS AND METHODS

All the reagents uses were of analytical grade all lanthanides salts were obtain from Sigma Aldrich. All solvents were used without further purification. The glass wares used were washed with detergent, rinsed with distilled water and dried in an oven at 110^0C before use.

The metal precursors used for the two products were cerium(lll) chlorides heptahydrate ($CeCl_3.7H_2O$) and Yttrium (lll) chlorides hexahydrate (YCl_36H_2O). Luteolin was used as the coordinating ligand. Ethanol and distilled water were used during synthesis, while dimethl sulfoxide (DMSO) used for measurements for which it was specified in the experiments. Characterization of the lanthanide-(III)-flavonoid complexes was carried out to confirm its successful coordination, elucidate the binding mode of the ligands (luteolin), determine physicochemical properties, and assess the structural stability of the complexes. A combination of spectroscopic, analytical, thermal, and magnetic techniques were employed to obtain comprehensive information on the complexes formed between Cerium(III) and Yttrium(III)- luteolin respectively.

The assessment of antimicrobial activities against selected a gram positive and a gram negative bacteria (*Bacillus subtilis* Gram-positive, and *Escherichia coli* Gram-negative) and two fungal strains *Candida*

ISSN No. 2321-2705 | DOI: 10.51244/IJRSI |Volume XIII Issue X October 2026

albicans and *Aspergillus niger* were all tested in the Department of Microbiology Laboratory Modibbo Adama University, Yola. Both Bacteriacidal and Fungicidal Adopted the methord used by (Gonelimali, *et al*., 2018).

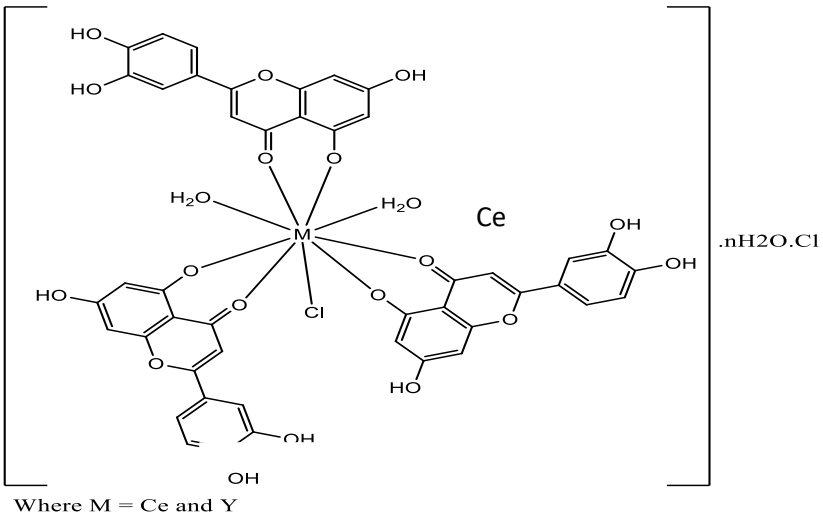
Synthesis of Cerium(III) and Ytrrium(III)-Luteolin Complexes

For each complex preparation, the appropriate metal salt was dissolved in 20 mL of distilled water, while the required amount of luteolin was dissolved separately in 40 mL of ethanolmetal-to-ligand molar ratio of 1:3. The metal salt solution was then added gradually to the luteolin solution in a beaker with continuous stirring. The initial pH was 4.2 to 4.6 and was adjusted to approximately 6.9 by dropwise 0.1 M sodium hydroxide. The mixture was refluxed for 3h with continuous stirring. After refluxing, the reaction mixture was concentrated to approximately half of its original volume. The resulting solid product was collected by filtration, washed twice with 10ml with distilled water and ethanol and dried in a desiccators over calcium chloride desiccant ($CaCl_2$) for three days until a complex crystal was obtained as used by (Gao, *et al* 2026).

Equation of the Reaction

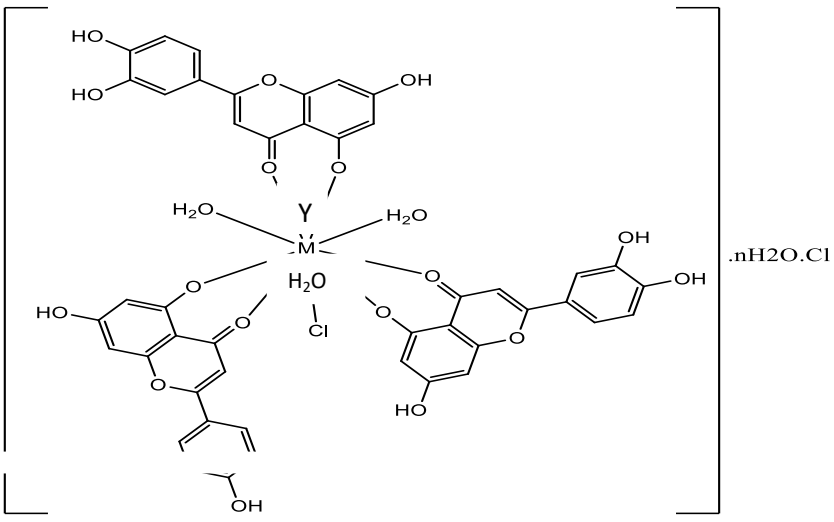
$$Ln(Cl)_3.6H_2O + 3C_{15}H_{10}O_6 + 3NaOH \xrightarrow{H_2O/EtOH/78^0C/pH\ 6.9} Ln(C_{15}H_{10}O_6)_3$$

$$+(NaCl)_3 + 9H_2O$$



Where M = Ce and Y

Figure 2: Proposed Structures of the Synthesized complexe of Ce



Where M = Ce and Y

Figure 3: Proposed Structures of the Synthesized complexe of Y

ISSN No. 2321-2705 | DOI: 10.51244/IJRSI |Volume XIII Issue X October 2026

Characterization Of The LigandAnd Its Synthesized Complexes *Percentage Yield*

The percentage yield of the synthesized metal-luteolin complexes was determined by comparing the experimental mass of the dried complex obtained after drying with the theoretically calculated mass of the complex expected from the Stoichiometric reaction using the relation below which adopted by (Tiwari,*et al.* 2023). The percentage yield was calculated using the formula;

$$\%\, Yield = \frac{Experimental\ yield}{Theoretical\ yield} *100$$

Solubility Studies

The solubility studies of the synthesized complexes and the free luteolin ligand were carried out qualitatively in six different solvents comprising aqueous and non-aqueous solvents of varying polarity. The solvents used were distilled water, methanol, ethanol, n-hexane, dimethyl sulfoxide (DMSO), and acetone. Approximately 0.01 g of each sample was separately and introduced into 2ml for each solvent in a test tube and observed at room temperature for about 10 minutes. The dissolution behavior of each sample was recorded. Samples that remained insoluble at room temperature were subsequently subjected to elevated temperature (approximately 50 °C) and re-examined to determine whether heating enhanced their dissolution. This approach was adopted with reference to the solubility investigation of metal complexes reported by Adamu, U. A.,*et al*. (2020).

Fourier Transform Infrared (FT-IR) Spectroscopy

The FT-IR spectra of free luteolin and the synthesized lanthanide(III) complexes was recorded in the range of 550-4000 cm^{-1} using the KBr pellet method.

The spectra examine the bands associated with the phenolic O-H stretching, carbonyl (C=O) stretching, and aromatic (C=C) vibrations. Changes in the O-H and C=O regions together with bands in the low frequency region, were considered as possible evidence of Metal- Oxygen interactions. These assignment are interpreted as supporting evidence of coorination of ligand and the metal ions as done by (Silverstein,*et al*., 2014).

Determination of Melting Point/Decomposition Temperature

The melting point/decomposition temperature of luteolin and its synthesized metal(III) complexes was determined using an OptiMelt melting point apparatus. A small quantity of finely powdered of each sample was packed into a clean capillary tube and inserted into the sample holder of the instrument. The instrument was programmed to heat the samples gradually from room temperature until complete decomposition while the samples were continuously observed. The temperature at which each sample first showed a visible colour change (the onset of decomposition) and The temperature at which it was completely decomposed were recorded as reported by (Fetouh, H. A., 2024).

Ultraviolet–Visible (UV–Vis) Spectroscopy

Ultraviolet–Visible (UV-Vis) spectroscopy was employed to investigate the electronic transitions and ligand–metal interactions. The spectra were recorded in an DMSO solvent at stated concentration of 1×10^{-3} at room temperature. The ligand exhibited absorption bands associated with transitions within the flavonoid system. Upon complexation with lanthanide-(III) ions, shifts in these absorption bands are anticipated due to changes in the electronic environment of the ligand. These spectral changes will be attributed to ligand-to-metal charge transfer (LMCT) interactions, providing evidence for complex formation (Bünzli,*et al.*, 2016).

Molar Conductance Measurements

Molar conductance measurements of the complexes were carried by preparing a solution of each metal (lll) complexes (0.001mol/dm^3) in DMSO in a test tube and the electrode was inserted and the reading was recorded and calculated using a relation below

ISSN No. 2321-2705 | DOI: 10.51244/IJRSI |Volume XIII Issue X October 2026

$\nabla m = \frac{k \times 1000}{C}$ as reported by (Govindrajan, k., and Ramesh, M. (2021).

Magnetic Susceptibility Measurements

A magnetic susceptibility measurement was performed to investigate the magnetic behavior and oxidation state of the lanthanide ions in the complexes. Y has a $3d^{10}$ configuration and is expected to be diamagnetic while Ce has $4f^{1}$ configurations and expected to show paramagnetic behavior. These experimentally determined magnetic moment values will be compared with theoretical values expected for Ln^{3+} ions. The results was confirm that the lanthanide ions retain their $^{(+3)}$ oxidation state after coordination and it will provide insight into the coordination environment around the metal centers as reported by (Cotton, S.A 2024).

Thermogravimetric Analysis (TGA)

Thermogravimetric analysis (TGA) was used to evaluate the thermal stability, decomposition behavior, and presence of coordinated or lattice water molecules in the complexes. Initial mass losses are expected to correspond to the removal of physically adsorbed or coordinated water molecules, while subsequent stages will represent ligand decomposition. The final residue is anticipated to be the corresponding lanthanide oxide, confirming the trivalent oxidation state of the metal ions. The thermal stability data obtained will support the suitability of the complexes for antimicrobial and biomedical applications (Materazzi, *et al.*, 2012).

Elemental Analysis and Metal Content Determination

Elemental (CHN) analysis was carried out to determine the carbon, hydrogen, and nitrogen contents of the synthesized complexes. The experimental values was compared with theoretical values calculated from proposed molecular formulas to confirm stoichiometry and purity. Metal ion content was determined using atomic absorption spectroscopy (AAS) or inductively coupled plasma optical emission spectroscopy (ICP-OES). Agreement between experimental and calculated values will support the proposed metal-to-ligand ratios and molecular composition of the complexes (Skoog, *et al.*, 2018).

The percentage difference between the theoretical and experimental values was calculated using:

$$\%\text{Diff} = \frac{Theoretical - Experimental}{Theoretical} * 100$$

Powder X-Ray Diffraction (PXRD)

Powder X-ray diffraction (PXRD) analysis was carried out to determine the crystalline nature and phase purity of the synthesized complexes. The patterns of the complexes are expected to differ from that of free luteolin, indicating the formation of new solid phases. Changes in diffraction peak positions and intensities will confirm successful complexation and provide information on the structural organization of the complexes as reported by (West, A. R. 2017).

Antimicrobial Assessments

The study of the antimicrobial properties of the free luteolin ($C_{10}H_{15}O_6$) and its meta (III) complexes were assayed against two bacterial isolates one gram-positive and one gram-negative bacteria (*Staphylococcus aureus,* and*Escheria coli)* by the reported method (Gonelimali, *et al.*, 2018).The suspension of each microorganism was rubbed into the surface of solidified nutrient agger (N.A) already poured into petri dishes with swap stick. The stock solution was suitably diluted to get dilution of 100, 50, 25 and 12.5 ug/well of the ligand, and the metal complexes. Wells (6mmin diameter) were dug in the agar media with the help of sterile metallic borer. Ciprofloxacin 5ug/disc was used as controls.The wells were incubated immediately at 37^0C for 24 hours. Activities were determined by measuring the diameter of zones showing complete inhibition (mm) and comparing the values with the standard as done by (Gonelimali, *et al.*, 2018).

ISSN No. 2321-2705 | DOI: 10.51244/IJRSI |Volume XIII Issue X October 2026

The study of the antifungal properties of the free luteolin ($C_{10}H_{15}O_6$) and its metal (III) complexes were assayed against two (*Candida albicans*, and *autragelliusniger*) fungal strains. This process was also adapted from the established Gonelimali protocol (Gonelimali, *et al.*, 2018).

RESULTS AND DISCUSSION

Table 1. Physical Properties of the Ligand and its metal (lll) Complexes

Compound	**Color**	**Percentage Yield (%)**	**Meltingpoint/Decomposition^{0}CTemperature**
Ligand	Yellow	-	316
$[Ce(L)_3Cl(H_2O)_2]3H_2O$	Black	68.82	351
$[Y(L)_3.(H2O)_3].4H2O$	Light Brown	83.96	357

Ligand = $C_{15}H_{10}O_6$ (Luteolin)

Free luteolin was obtained as a yellow solid crystal while, and both$[Y(Cl)_3.6H2O]$ $[Ce(Cl)_3.7H_2O]$ are all white crystals. The percentage yields obtained for the synthesized complexes ranged from 68.82 to 83.96. for Ce and Y complexes respectively.

Luteolin was found having melting point of 316 °C. After complexation, the products differ in color from the ligand. Ce shows Black and Y is Light brown. The melting point of free luteolin was in accordance with the previous studies (Malacaria *et al*., 2022). Similarly melting points of the synthesized complexes was 351 ^{0}C for Ce and 357 ^{0}C Y. these temperatures were higher than that of free luteolin this increase suggests that the synthesized complexes have stronger intermolecular interactions and greater thermal stability than the ligand as reported by (Jayaprakash, S. 2023).

Solubility studies

Table 2 Solubility Results of the ligand and its metal(lll) complexes

Sample	**H20**	**Ethanol**	**Methanol**	**DMSO**	**Acetone**	**n-Hexane**
Ligand	IS	S	S	S	S	IS
$[Ce(L)_3Cl(H_2O)_2]3H_2O$	lS	SL	IS	S	IS	Ls
$[Y(L)_3(H_2O)_3].4H2O$	lS	S	S	S	SL	Is

Key: S=Soluble, Sl= Sligthly Soluble, Is =Insoluble. **L =** $C_{15}H_{10}O_6$ (Luteolin)

The solubility studies were carried out in six deferent (aqueous, polar and non-polar) solvents. The solubility results show that both ligand and its resulting complexes were insoluble in water and n-hexane, but generally dissolves better in polar organic solvents tested,although their solubility varied. All compounds are found soluble in DMSO, methanol except for Ce-Complex insoluble. Ethanol dissolves only Y-complex and Ce-Complexewere found slightly soluble. In acetone, only the ligand was soluble and Y-Complexeswere slightly soluble, while Ce-Complexwas the only insoluble. These differences could be due to variations in the metal ions, coordination environments, and structures of the complexes. The solubility results are in accordance with previous reports on the poor water solubility of luteolin(Rajhard S, *et al.*, 2021).

Fourier Transmittance infrared Results (FTIR)

Table 3 Infrared Spectral data of Ligand and its Metal(lll) Complexes

ISSN No. 2321-2705 | DOI: 10.51244/IJRSI |Volume XIII Issue X October 2026

Sample	***v*OH Stretching**	***v*C=O**	***v*M-O**	***v*M-OH$_2$**
Ligand	3198	1659	-	-
$[Ce(L)_3Cl(H_2O)_2]3H_2O$	3126	1651	596	628
$[Y(L)_3.(H_2O)_3]$.4H2O	3188	1653	560	623

Ligand = $C_{15}H_{10}O_6$ (Luteolin) **Analyzing band range**. 550-4000.

The FTIR spectra of luteolin and the synthesized metal complexes were recorded within the 550-4000 cm^{-1}range. Free luteolin showed a strong C=O stretching band at 1659 cm^{-1} and an O-H stretching band at 3198 cm^{-1}. The FTIR of its synthesized complexes reveals the C=O band shifted lower to 1651 cm^{-1} for Ce-Complex, and 1653 cm^{-1} for Y-Complex respectively.

The O-H bands for Ce and Y-complexes occurred within 3126 and 3188 cm^{-1}, respectively. Another new vibration bands appeared at 596 for Ce and 560cm^{-1}Y- complexes and were assigned to M-O vibrations. Similar changes in characteristic FTIR bands have been reported for flavonoid-metal complexes (Bamigboye*et al.* 2020) and (Edewor *et al.* 2023).

The changes observed in the C=O and O-H bands, together with the appearance of the M-O bands, provide evidence of metal-oxygen interaction and suggest possible O,O-chelation of luteolin. The 4-carbonyl and 5-hydroxyl region is a primary chelating site reported (Malacari a*et al.* 2022).

The bands observed between 628 cm^{-1} for Ce-complex and 623 $cm^{-1}$for Y-complex were assigned to M-OH_2 vibrations associated with coordinated water molecules. This assignment agrees with the findings of M. M. El-Zahed, *et al.* (2025), who reported M-O vibrations in the 617-655 cm^{-1} regions, along with bands associated with the wagging and rocking modes of coordinated water.

The presence of chloride in $[Ce(L)_3Cl(2H_2O)]3H_2O$, complex was confirmed by elemental analysis**.** However, because the FTIR spectra in this study were recorded in the range of 550-4000 cm^{-1}vibrations occurring below550 cm^{-1} could not be directly observed. This limitation is particularly relevant when considering the M-Cl stretching vibrations, which typically appear in the region 321 to 328 cm^{-1}as reported by (Muraleedharan *et al*., 2025). And equally Dy-Cl vibration bands at approximately 234 and 221 cm^{-1} were observed as reported by (Persaud, *et al*., 2024). This indicates that lanthanide-chloride vibrations can occur at considerably lower wavelengths than the lower limit used in this study.

The FTIR results support the formation of the $[Ce(L)_3Cl(H_2O)_2]3H_2O$,and $[Y(L)_3.(3H2O)]$.4H2O. Complexes and suggest that luteolin coordinates with the metal ions through oxygen donor atoms.

UV Visible Results Spectral Analysis of Luteolin And Its Metal(Iii) Complexes

ISSN No. 2321-2705 | DOI: 10.51244/IJRSI |Volume XIII Issue X October 2026

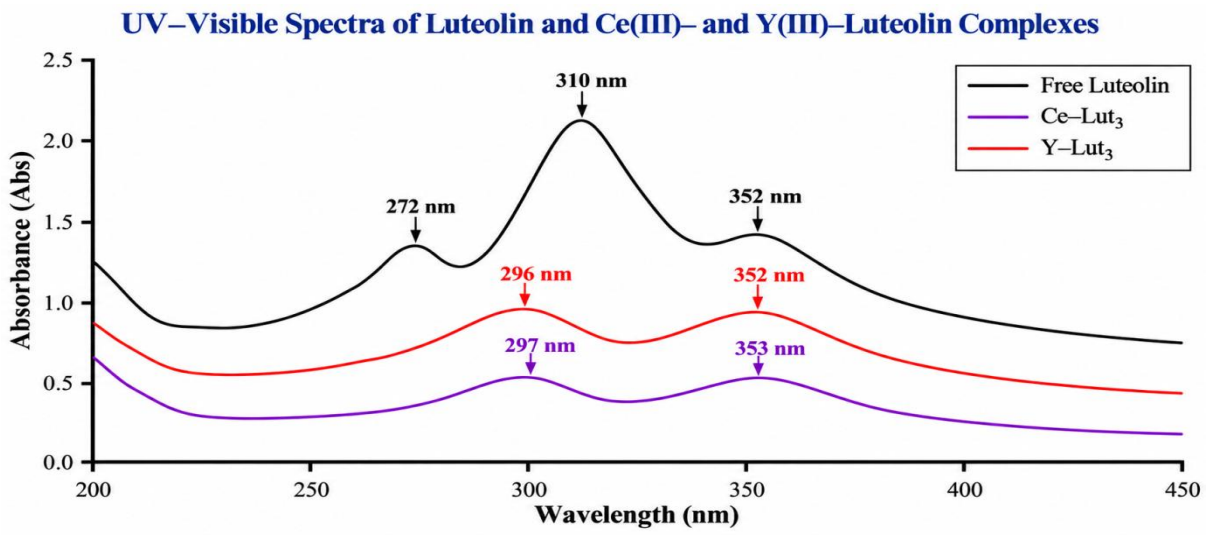


Figure 3: UV visible ResultsSpectral Analysis of Luteolin and Its Metal(III) Complexes

The UV-Visible spectra of free luteolin and its synthesized metal-(III)-complexes in table4.4 showed two main absorption bands. Free luteolin gave absorption maxima at 272 and 310 nm in DMSO. These values are close to the 271 and 353 nm as reported for luteolin in DMSO by Tawornchat *et al.* (2021).

After the metal ions were introduced to the ligand, changes were observed in the absorption bands of luteolin. The first band at 272 nm in free luteolin shifted to296 nm for Y-Complex, 297 nm for Ce-Complex. Band ll of the free luteolin shifted from 310 to 352 nm for Y-Complexand 353 nm for Ce-Complex Similar changes have been reported for luteolin following its interaction with metal ions (Malacaria *et al.*, 2022).

Molar Conductance Of The Complexes.

Table 4 Molar Conductance Results

Complex	**Conductance** $\mu s/Cm^{-1}$	**Specific Conductivity** Ohm^{-1} Cm^{-1}	**Molar Conductivity** Ohm^{-1} Cm^{-1} Mol^{-1}	**Electrolytic Nature**
[Ce(L)3Cl(H2O)2].3H2O	155	$1.55x10^{-4}$	1.55	Non-Electrolyte
[Y(L)3. (H2O)3].4H2O	86	$8.6\ x10^{-5}$	8.60	Non-Electrolyte

The Table above presents the results of molar conductivity measurements of the synthesized complexes. Conductivity was measured at room temperature, using DMSO solvent at a concentration of 1×10^{-3} M. The complexes recorded molar conductivity values was 1.55 Ω^{-1} cm² mol^{-1} for Ce-complex and 8.60 Ω^{-1} cm² mol^{-1} Y-complex and These relatively low values are consistent with the behavior generally observed for non-electrolytic coordination complexes. Similarly, this values agrees with the reported studies (Dongare and Aswar 2021).

This suggests that the complexes exist mainly as neutral complexes in solution, with little contribution from freely mobile counter-ions.

Thermogravimetric Stability Analysis Tga–Dtg Results

Thermogravimetric Analysis (TGA) were utilized to evaluate the thermal stability and decomposition profiles of the synthesized materials.TGA monitors the continuous weight loss of a sample as a function of temperature under a controlled atmosphere, providing sharp, distinct peaks that pinpoint the exact temperatures of maximum decomposition and precise identification of distinct thermal degradation steps-such as moisture

ISSN No. 2321-2705 | DOI: 10.51244/IJRSI |Volume XIII Issue X October 2026

desorption, volatile evolution, and establishing a foundational understanding of the material's thermal behaviour and structural composition.

Table 5; TGA $[Y(L)_3(H_2O)_3].4H2O$ complex

Stage	**Temperature Range (^oC)**	**Weight loss (%)**	**Peak DTG (%min)**	**Possible Assignment**
1	30-150	5.4	0.90	Loss of 4 Lattice H_2O Molecules
2	150-280	4.65	0.715	Loss of 3 Coordinated H_2O molecules
3	280-430	78.25	10.433	Decomposition of organic moiety.
4	430-600	-	-	Formation of stable metal oxide residue

Remaining 11.69% Metal Oxides Residue

Table 6; TGA $[Ce(L)_3Cl(H_2O)_2].3H_2O$ -Complex

Stage	**Temperature Range (^oC)**	**Weight loss (%)**	**Peak DTG (%min)**	**Possible Assignment**
1	30-150	4.89	0.82	Loss of 3 Lattice H_2^0 Molecules
2	150-280	3.26	0.50	Loss of 2 Coordinated H_2^0 molecules
3	280-430	79.62	10.616	Decomposition of organic moiety + loss of one coordinated lonic Cl as HCl
4	430-600	-	-	Formation of stable metal oxide residue

Remaining 12.23% Metal Oxides Residue

Decompositions in first stage occur between the temperature 30-150 °C. There are weight loss of 4.89 - 5.40% from the complexes and are attributed to the removal of lattice water loss within thisdehydration region. loss of water is commonly observed in hydrated metal complexes during thermal analysis repotted (Iorungwa *et al.*, 2024).

The second stage temperature range between 150-280 °C. Weight loss for all complexes was observed and these losses are considerably lower than those recorded during the main decomposition stage of 3.26 to 4.65% suggesting that water is removed (coordinated). A similar sequence of dehydration followed by ligand decomposition has been reported for metal complexes by (Iorungwa*et al.*, 2024).

The third stage is the major decomposition stage and accounts for the largest proportion of mass loss of organic moiety in all of the four complexes. It occurs between 280-430 °C temperature range. The weight loss are huge in between 78.25 to 78.62 %, These results indicate extensive degradation of the organic component and some minor inorganics of the complexes. Similarly a pronounced ligand-decomposition recorded highest mass loss. This is in accordance with reported Thermogravimetric studies of metal complexes by (Fabiyi and (Olanrewaju, 2019).

Stage four is the final stage at extended temperature range s 430 to 600 °C, The residues remaining at the end of the analysis observed ranges 11.69 – 12.23 % of the stable Metal oxides. Similar use of residues in assessing the inorganic fraction of metal complexes has been reported by Ama *et al.* (2024). The thermal profiles indicate a progressive decomposition pathway involving loss of lattice water, removal of coordinated

ISSN No. 2321-2705 | DOI: 10.51244/IJRSI |Volume XIII Issue X October 2026

water, degradation of the organic moiety and other impurities and finally formation of stable inorganic residues.(Iorungwa*et al.,* 2024).

The Magnetic Susceptibility Of The Metal (Iii) Complexes

Table 7; The Magnetic Moments of the metal (lll) complexes are

Complex	**(R-Ro)**	**Xg Cm^3/g**	**Xm Cm^3/Mol**	***μ*eft(BM) (Bm)**	**Property**
$[Ce(L)_3Cl(H_2O)_2].3H_2O$	44	$7.8107x10^{-7}$	$8.2337x10^{-4}$	1.40	Paramagnetic
$[Y(L)_3.(H_2O)_3].4H_2O$	-	-	-	Dia	Diamagnetic

The magnetic moments of the synthesized complexes shows that Ce-complexes is paramagnetic while Y-complex is Diamagnetic in Nature. The magnetic moments of the complexes are in good agreement with the expected values as reported by (Haruna *et al*. 2024), (Mortis D, *et al.,* 2024) and while Diamagnetic behavior of Y-complex is in accordance with the findings of (Bera S.P. *et al.,* 2022).

Elemental Analysis Of The Theoretical/Experimental Results

Elemental analysis was carried out to determine the presence and composition of each element in synthesized metal (lll) luteolin complexes and to compare with experimental values with the theoretical values calculated from their proposed compositions as presented in table 8 to 9 below

Table 8; $[Y(L)_3.(H_2O)_3].4H_2O$

Element	**Theoretical %**	**Experimental %**
Y	11.88	10.80
C	50.76	50.75
O	33.64	33.87
H	3.62	3.59
Cl	0.10	0.99

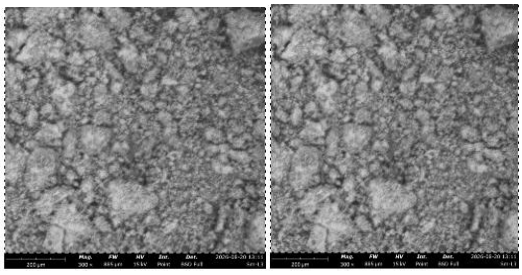


Table 9; $[Ce(L)_3Cl(H_2O)_2].3H_2O$ Complex

Element	**Theoretical %**	**Experimental %**
Ce	13.21	12.97
C	51.44	50.39

ISSN No. 2321-2705 | DOI: 10.51244/IJRSI |Volume XIII Issue X October 2026

O	31.71	31.44
H	3.44	3.27
Cl	0.20	1.93

Metal (III) ions

The experimental metal contents of the Ce-complex is 12.97%, compared with theoretical values of 13.21%. The percentage differences 0.24%. Ce(III) showed the smallest difference from its theoretical value, while Y(III) showed experimental metal contents of 10.80%, compared with theoretical values of 11.88%.with the largest percentage difference of 1.08%This result is consistent with the findings of (Pospieszna-Markiewicz *et al.* 2022).

Carbon

The experimental carbon contents of the Ce-complex is 50.39%, while the theoretical value of 51.44% and percentage difference of 1.05%. While Y(III)-complex showed the experimental carbon content 50.75% and theoretical value of 50.76% The percentage difference of 0.01%. These were reported by (Walencik *et al.*, 2024).

Oxygen

The experimental oxygen contentsof the Ce-complex is 31.44%, compared with theoretical values of 31.71%. The percentage difference of 0.27% While Y(III)-complex showed the experimental carbon content 33.87% and theoretical value of 33.64%The percentage difference of 0.23% This close agreement between the experimental and theoretical oxygen contents indicates that the oxygen-rich nature of luteolin is reasonably represented in the synthesized complexes. This is significant because luteolin contains several oxygen-containing functional groups capable of participating in metal coordination. (Walencik *et al*. 2024).

Hydrogen

The experimental hydrogen contents of the Ce-complex is 3.27%, compared with theoretical values of 3.44%. The percentage differences of 0.17%.While Y(III)-complex showed the experimental Hydrogen content 3.59 % and theoretical value of 3.62%The percentage difference of 0.03% The experimental hydrogen values were slightly lower than the theoretical values for all the complexes. The relatively small and consistent differences may be associated with differences in hydration, drying conditions, sample composition and analytical variation. This is particularly relevant to lanthanide complexes because hydrated species can occur in the isolated products. (Matsia *et al.*2025).

Chlorine

Chloride contents was detected in $[Ce(L)_3.Cl.2H_2O].3H_2O$ with 1.93%, experimental, compared with theoretical values of 0.20%. The percentage differences of 1.73%.While $[Y(L)_3.3H_2O].4H_2O$ complexes was detected with experimental values of 0.99%, and theoretical 0.10% with percentage difference of 0.89%. The small chlorine signals in $[Ce(L)_3.Cl.2H_2O].3H_2O$ and $[Y(L)_3.3H_2O].4H_2O$ is associated with the chloride salts used during synthesis ($CeCl_3 \cdot 7H_2O$ and $YCl_3 \cdot 6H_2O$) (Manvell, *et al* 2024) and (Khorasani-Motlagh, *et al.*,(2013).

Xrd Diffraction Pattern Of The Synthesized Complexes

The figure 5 below presents the results and analysis of the combine X-ray diffraction (XRD) measurements conducted to evaluate the structural properties, phase purity, and crystallographic configurations of the synthesized samples. To establish a rigorous foundation for the structural characterization, the obtained

ISSN No. 2321-2705 | DOI: 10.51244/IJRSI |Volume XIII Issue X October 2026

experimental diffraction patterns were systematically analyzed and indexed against standard reference databases XRD match-4-Software.

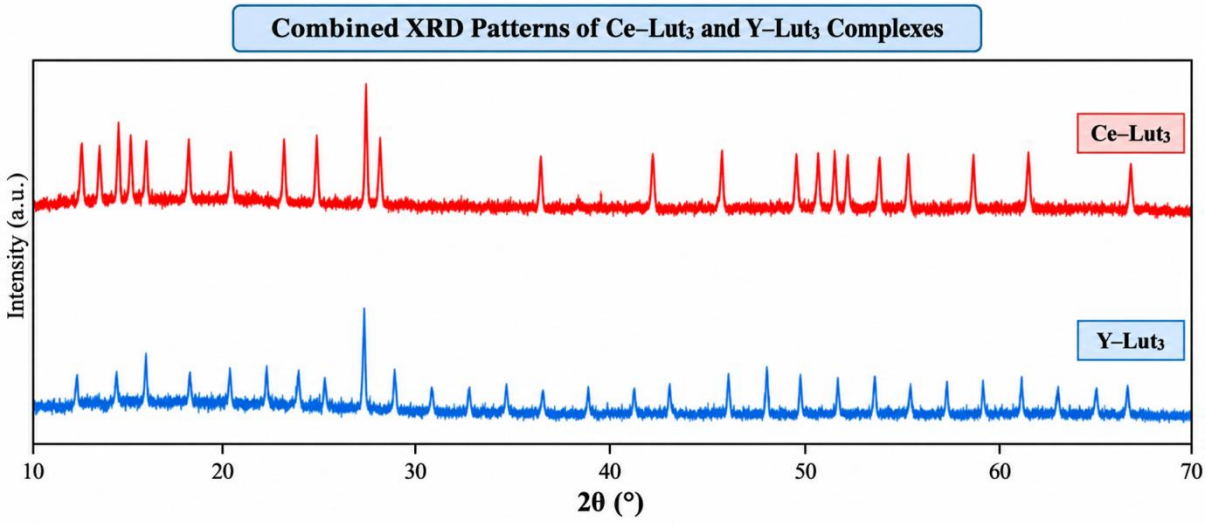


Figure 5 combine XRD Results

The XRD pattern of the synthesized $[Y(L)_3.(H_2O)_3].4H_2O$. Clcomplex displayed several reflections across 2θ range of 10-70° The most prominent peak among was observed at 28.26°, with an intensity of 59.6 counts and a d-spacing of 3.1568 (Å). The complex is in the range ($<70^0$) indicating is a crystalline complex and the corresponding d-spacing demonstrates structural orderings within the complex (Holder *et al* 2019). Jafar *et al. (*2021) reported that Luteolin exhibit characteristic crystalline reflections around 14.3°, 16.1°, 26.1°, 27.6° and 29.2°. Y(lll) complex shows with predominantly hexagonal (Graphite/Cronusite-type) phases and crystallite size about 850±13Å.

The XRD pattern of the synthesized $[Ce(L)_3.Cl.2H_2O].3H_2O$ complex was examine to determine its diffraction characteristics such as crystallinity and phase characteristics. A numerous sharp diffraction peaks in the 2θ range of $10\text{-}70^0$ with the strongest peak at 37.95° (75counts) and d-spacing of 2.3690 (Å). The complex is in the range ($<70^0$) indicating is a crystalline complex and the corresponding d-spacing demonstrates structural orderings within the complex (Holder *et al* 2019). The relatively broad peaks or noisy background indicates moderate crystalline material. The diffraction pattern differs from the characteristic crystalline pattern reported for free luteolin (*Jafar et al.* 2021). These indicate modification of the ligand's solid-state packing. Ce-complex shows with predominantly hexagonal (Fluocerite/-type) phase respectively. The complex exhibited crystallite size about 810±215Å, which is consistent with Scherrer equation calculation.

Antimicrobial Studies

Table 10 ; Antibacterial activity of luteolin, its metal complexes and control

TEST-MATERIAL	**CONCENTRATION**	**S. aurius**	**E. coli**
$[Ce(L)_3.Cl.2H_2O].3H_2O$	100	15	15
$[Ce(L)_3.Cl.2H_2O].3H_2O$	50	13	14
$[Ce(L)_3.Cl.2H_2O].3H_2O$	25	12	10
$[Ce(L)_3.Cl.2H_2O].3H_2O$	12.5	10	8
$[Ce(L)_3.Cl.2H_2O].3H_2O$	6.25	9	7

ISSN No. 2321-2705 | DOI: 10.51244/IJRSI |Volume XIII Issue X October 2026

$[Ce(L)_3.Cl.2H_2O].3H_2O$	3.12	6	7
$[Y(L)_3.3H_2O].4H_2O$	100	14	15
$[Y(L)_3.3H_2O].4H_2O$	50	13	10
$[Y(L)_3.3H_2O].4H_2O$	25	9	10
$[Y(L)_3.3H_2O].4H_2O$	12.5	NZ	NZ
$[Y(L)_3.3H_2O].4H_2O$	6.25	NZ	NZ
$[Y(L)_3.3H_2O].4H_2O$	3.12	NZ	NZ
Ligand	100	14	14
Ligand	50	12	12
Ligand	25	9	7
Ligand	12.5	NZ	NZ
Ligand	6.25	NZ	NZ
Ligand	3.12	NZ	NZ
Control	100	32	32
Control	50	28	29
Control	25	28	24
Control	12.5	26	20
Control	6.25	20	17
Control	3.12	10	10

Ligand = $C_{15}H_{10}O_6$ (Luteolin)

Control = Ciprofloxacin

Concentration used = (μg/mL)

Inhibition-Zone diameter = (mm)

Table 11; Antifungal activity of luteolin, its metal complexes and control

TEST-MATERIAL	**CONCENTRATION**	**A. niger**	**C. albicans**
$[Ce(L)_3.Cl.2H_2O].3H_2O$	100	10	18
$[Ce(L)_3.Cl.2H_2O].3H_2O$	50	6	10
$[Ce(L)_3.Cl.2H_2O].3H_2O$	25	NZ	8

ISSN No. 2321-2705 | DOI: 10.51244/IJRSI |Volume XIII Issue X October 2026

$[Ce(L)_3.Cl.2H_2O].3H_2O$	12.5	NZ	8
$[Ce(L)_3.Cl.2H_2O].3H_2O$	6.25	NZ	NZ
$[Ce(L)_3.Cl.2H_2O].3H_2O$	3.12	NZ	NZ
$[Y(L)_3.3H_2O].4H_2O$	100	12	16
$[Y(L)_3.3H_2O].4H_2O$	50	8	8
$[Y(L)_3.3H_2O].4H_2O$	25	NZ	6
$[Y(L)_3.3H_2O].4H_2O$	12.5	NZ	NZ
$[Y(L)_3.3H_2O].4H_2O$	6.25	NZ	NZ
$[Y(L)_3.3H_2O].4H_2Ol$	3.12	NZ	NZ
Ligand	100	10	16
Ligand	50	6	8
Ligand	25	NZ	4
Ligand	12.5	NZ	NZ
Ligand	6.25	NZ	NZ
Ligand	3.12	NZ	NZ
Control	100	30	30
Control	50	26	26
Control	25	19	20
Control	12.5	16	10
Control	6.25	10	8
Control	3.12	NZ	6

Lgand = $C_{15}H_{10}O_6$ (Luteolin)

Control = Ketoconazole

Concentration = (μg/mL)

Inhibition-Zone diameter = (mm)

The bacteriacidal and fungicidal results in Table 10 and 11 respectively below showed that luteolin and all its resulting synthesized complexes $[Ce(L)_3.Cl.2H_2O].3H_2O$, and $[Y(L)_3.3H2O].4H2O$, showed antibacterial activity against both Gram-positive and Gram-negative isolates(*Staphylocuccus Aureus* and *Eschericia Coli)* and sensitivity to yeast and mould fungi (*Candida albicans* and *Asperigellusniger*) tested respectively. The antimicrobial activity was assayed using inhibition-zone measurements at different concentrations, and a volume of 0.2ml was used for each complex. The results shows that both the ligand and its complexes

possesses biological activity concentration depended. The results also revealed that the activity of the ligand is enhanced by the coordination to a metal ions but less than the standard used this observation is consistence with findings from Nigerian researchers, including (Andrew *et al*. 2023).

CONCLUSION

The study successfully synthesized $Ce(L)_3.Cl.2H_2O].3H_2O$ and [Y(L)3.3H2O].4H2O-complexes of luteolin, and characterized them using physicochemical, spectroscopic, magnetic, thermal, elemental and X-ray diffraction techniques. The FTIR results support particularly the changes in the O-H and C=O vibrations and the appearance of M-O bands, together with the UV–Visible and other characterization results, supported the formation of the complexes. The XRD results indicated crystalline products, while the antimicrobial studies demonstrated antibacterial and antifungal activities of varying degrees. Based on the combined characterization results, the complexes are proposed to possess an O,O-chelating involving the oxygen donor sites of luteolin, particularly the carbonyl and hydroxyl groups. And coordination with predominantly hexagonal Graphite-like geometry.

REFERENCES

1. Adamu, U. A., Magaji, B., Mohammad, A. B., Sani, M. M., and Adoram, N. (2020). Synthesis, characterization and antibacterial study of Co(II) and Cu(II) complexes of sulfamethoxazole. Asian Journal of Advanced Research and Reports, 10(4), 38-43. https://doi.org/10.9734/ajarr/2020/v10i430251.
2. Ama, S. O., Wuana, R. A., Sha'ato, R., and Eneji, I.S. (2024). Green synthesis, structural characterization and study of thermal behavior of Cu^{2}' and Co^{2}' complexes derived from salicylidene-3-amino benzoie acid African Multidisciplinary Journal of Sciences and Artificial Intelligence. 1.620 633. Article source.
3. Andrew,S.Z.,Japhet,T.,Bako,B.,Abakpa,A.M.,&Shinggu,J.P.(2023).Synthesisandpreliminaryantibacterialscreeningofsalicylaldehyde aminobenzoic acid anditsmetalcomplexe.10(3),40–46.
4. Bamigboye, O. M., Ejidike, I. P., & Lawal, M. (2020). Synthesis, characterization, and antimicrobial potentials of some flavonoid–metal complexes. Iraqi Journal of Science, 61(4), 789–799.
5. Bünzli, J.-C.G., and Pecharsky, V. K. (2016).Handbook on the Physics and Chemistry of Rare Earths.Elsevier.
6. Bera, S. P., Mondal, A., and Konar, S. (2022). Investigation of the role of terminal ligands in magnetic relaxation in a series of dinuclear dysprosium complexes.Inorganic Chemistry Frontiers, 7(18), 3352–3363. doi.org
7. Bonetti F, Brombo G, Zuliani G (2017) Nootropics, functional foods, and dietary patterns for prevention of cognitive decline. In: Watson RR (ed) Nutrition and Functional Foods for Healthy Aging. Academic Press, Cambridge, pp 211 –232.
8. Cotton, S. A. (2024). Lanthanide and Actinide Chemistry, 2nd ed.; Wiley, susceptibility and tetracycline-resistance gene distribution. Microb Pathog.2017;105:51–56. doi:10.1016/j.micpath.2017.02.010
9. Dongare, G., and Aswar, A. (2021). Synthesis, spectral characterization, thermo-kinetic and biological studies of some complexes derived from tridentate hydrazone Schiff base. Journal of Saudi Chemical Society, 25(10), 101325. doi.org.
10. Edewor, T.I., Bankole T.A., Ogunjimi, D.V., Mmuo, A.I., & Amuda, M.O. (2023). GC-MS profile, synthesis and speetral characterization of flavonoid-metal (cadmium, cobalt, copper, nickel) complexes of Jatropha curea leaves International Journal of Chemistry Research, 7(2).4 12.IJCR.1.
11. Fabiyi, F. S., and Olanrewaju, A. A. (2019). Synthesis, characterization, Thermogravimetric and antioxidant studies of new Cu(II), Fe(II), Mn(II), Zn(II), Co(II) and Ni(II) complexes with benzoic acid and 4,4,4-trifluoro-1-(2-naphthyl)-1,3-butanedione. International Journal of Chemistry, 11(1), 60–70. doi.org
12. Fetouh, H. A., Dissouky, A. E., Salem, H. A., Fathy, M., Anis, B., & Hady Kashyout, A. E. (2024). Synthesis, characterization and evaluation of new transition metal complexes of luteolin derivatives.

Journal of Molecular Structure (or alternate specific journal depending on exact volume, such as Scientific Reports / MDPI Advances in Phenolic Based Complexes). [1, 2

13. Gao, W., Pan, L. S., Lei, L., and Zhu, C. (2026). Synthesis, characterization and antioxidative activity of lanthanide complex with luteolin.Chemical Journal of Chinese Universities, 44(4), 663–665.Górniak, I., Bartoszewski, R. &Króliczewski, J. (2019).Comprehensive reviewof antimicrobial activities of plantfavonoids.Phytochem. Rev. 18, 241–272.
14. Gonelimali, FD, Lin J, Miao W, Xuan J, Charles F, Chan M, Hatab SR.(2018). Antimicrobial properties and mechanisms of action of some plant extracts against food pathogens and spoilage microorganisms. Frontiers in microbiology.
15. Govindrajan, K., and Ramesh, M. (2021). Design, synthesis, characterization and biological activities of some transition metal complexes via novel mannich base ligand. International Journal of biology, Pharmacy and Allied Sciences (IJBPAS), 117p137.
16. Giuseppina Anna Corrente, G. A., Luana Malacaria, Amerigo Beneduci, TizianaMarino, and Emilia Furia, (2025). Quercetin and luteolin complexation with first-row transition metalsin purely aqueous solutions Stoichiometry and binding siteselectivity.DaltonTransactions,54(19), 7828–7837. https://doi.org/10.1039/D5DT00478K.
17. Haruna, M., Ndahi, J. A., Dowell, B. F., &Sadauki, F. T. (2024). Synthesis, physicochemical and antimicrobial studies of Schiff base derived from 2,4-dinitrophenylhydrazine with salicylaldehyde and its Co(II) and Ni(II) complexes. IDOSR Journal of Scientific Research, 9(2), 112. https://doi.org/10.59298/IDOSRJSR/2024/9.2.1211.10.DoSR+1.
18. Holder, C. F., Schaak, R. E., (2019).tutorial on power x-ray Diffraction for characterizing materials. ACS publication https.doi.org/10.1021/acsnano.
19. Iorungwa, M. S., Dafa, S. T., Wuana, R. A., Iornumbe, E. N., & Tivkaa, J. T. (2024). Thermal stability profiling of Co(II), Mn(II), and Ni(II)-Hydrazone Based complexes: The role of kinetic and thermodynamics parameters. ChemSearch Journal, 14(2), 46–57. https://www.ajol.info/index.php/csj/article/view/262735 [1]
20. Jafar,M.,Salahuddin,M.,Khan,M.S.A., Alshehry , Y., Alrwaili, N.R., Alzahrani, Y. A., Imam S. S., and Alshehry, S.(2021).Preparation and In Vitro-In-Vivo Evaluation of Luteolin Loaded GastroretentiveMicrosponge for the Eradication of Helicobacter pylori Infections. Pharmaceutics 13.(12), 2094. https;doi.org/10.33290.
21. Jayaprakash, S., Ramesh, S., Karthikeyan, A., Murugappan, S., Sidharthan, P., and Selvaraj, S. (2023). Transition metal coordination complexes of flavonoids: A class of better pharmacological active molecules to develop new drugs. Anti-Cancer Agents in Medicinal Chemistry, 23(4).417-431.
22. Kumar, P., Singh, R., & Mehta, A. (2021). Flavonoid-metal interactions: Implications for bioactivity. Bioinorganic Chemistry Applications, 2021, 1-12.
23. Khorasani-Motlagh M, Noroozifar M, Moodi A, Niroomand S. (2013).Journal of Photochemistry and Photobiology B: Biology 127, 192-201.
24. M. M. El-Zahed, A. A. El-Bindary, N. M. Mansour, H. M. Salama and Sh. M. Morgan (2025). Design, antibacterial activity, DNA interaction, anticancer and molecular docking analysis of novel bivalent metal chelates based on an N,O-donor Schiff base ligand. Discover Materials.Springer.
25. Malacaria, I.,,I.a Torre. C., Furia, F., Fazio, A., Caroleo. M.C., Cione. F., Gallelli, I. Marino, T., &Plastina, P. (2022). Aluminum (III), iron (III) and copper (II). Complexes of Luteolin: Stability, antioxidant, and anti-inflammatory properties. Journal ofMolecular Liquids, 345.117895. https://doi.org/10.1016/j.molliq.2021.117895. Science Direct.
26. Manvell, A. S., Pfleger, R., Bonde, N. A., Briganti, M., Mattei, C. A., Nannestad, T. B., Weihe, H., Powell, A. K., Ollivier, J., Bendix, J., & Pedersen, K. S. (2024). LnDOTA puppeteering: Removing the water molecule and imposing tetragonal symmetry. Chemical Science, 15(1), 113–123. doi.org
27. Materazzi, S., Vecchio, Ciprioti, S., Wo, L. W., and De-angelis Curtis.,(2012).TG-MS and TG-FTIR studies of immidazole substituted coordination compounds Co(ll) and Ni(ll) complexes bis(1-methylimmidazole-2-yl)ketone thermochimica Acta 543-183-187.
28. Matsia, S., Papadopoulos, A., Hatzidimitriou, A., Schumacher, L., Koldemir, A., Pöttgen, R., Panagiotopoulou, A., Chasapis, C. T., &Salifoglou, A. (2025). Hybrid Lanthanide Metal–Organic Compounds with Flavonoids: Magneto-Optical Properties and

Biologica Activity Profiles. International Journal of Molecular Sciences, 26_(3), 1198. https://doi.org/10.3390/ijms26031198[1].

29. Mortis, A., & Anwander, R. (2024). Rare-earth-metal alkyl and aryl compounds in organic synthesis. European Journal of Inorganic Chemistry, 27(16), e202400127. doi.org
30. Muraleedharan, Jincy Ennakkathara; Viswanathan, Kaladharan Perumpaparampil (2025). Microwave Assisted Synthesis of Some Ln(III) Chloride Complexes from 4-Formyl Antipyrine Schiff base: Structural Characterization and Antimicrobial Evaluation. Published in: Oriental Journal of Chemistry, 2025, v. 41, n. 1, p. 254, doi. 10.13005/ojc/410130
31. Persaud, A. A., Sasidharanpillai, S., Cox, J. S., and Tremaine, P. R. (2024). Speciation and formation constants of aqueous lanthanum(III) chloride complexes from 5 to 80 °C by Raman spectroscopy. Canadian Journal of Chemistry, 102(12), 922–934. doi.org ScienceDirect.com.
32. Pospieszna-Markiewicz, I., Fik-Jaskółka, M. A., Hnatejko, Z., Patroniak, V., & Kubicki, M. (2022).Synthesis and Characterization of Lanthanide Metal Ion Complexes of New Polydentate Hydrazone Schiff Base Ligand._Molecules, 27(23), 8390. https://doi.org/10.3390/molecules27238390[3].
33. Rajhard, S.; Hladnik, L.; Vicente, F.A.; Srčič, S.; Grilc, M.; Likozar, B. (2021). Solubility of Luteolin and Other Polyphenolic Compounds in Water, Nonpolar, Polar Aprotic and Protic Solvents by Applying FTIR/HPLC. Processes 2021, 9 (11), 1952. [1]
34. Sabrina, Coprali., Alesandro, De Stefano., Cinzia, Calabrese., Alfredo, Giovannelli., Massimo, Pieri., IsabelDy,Savini., Manfredi, Tesauro., Sergio, Bernardini., Marilena, Mineri., Alesandro, Terrinoni (2022). Anti-Inflammatory and Active Biological Properties of the Plant-Derived Bioactive Compounds Luteolin and Luteolin 7-Glucoside.National Library ofMedicine USA.
35. Silverstein, R. M.; Webster, F. X.; Kiemle, D. J.; Bryce, D. L.(2014). Spectrometric Identification of Organic Compounds, 8th edition.; Wiley,.structural aspects. Coordination Chemistry Reviews.
36. Skoog, D. A., Holler, F. J., and Crouch, S. R.(2018.). Principles of Instrumental Analysis, (7th ed). Cengage Learning.
37. Tawornchat, P., Pattarakankul, T., Palaga, T., Intasanta, V., &Wanichwecharungruang, S. (2021). Polymerized luteolin nanoparticles: Synthesis, structure elucidation, and anti-inflammatory activity.ACS Omega, 6(4), 2846 2855. https://doi.org/10.1021/acsomega.0c05142
38. Tiwari, L., and Waynant, K. V. (2023). The synthesis and structuralproperties of a chloridobis{N [(4me thoxyphenyl)imino]pyrrolidine1carboxamide}zinc(II)(acetonitrile)trichlordozincate coordination complex. Journal of Coordination Chemistry, 76(11–12), 1435–1448. doi.org.
39. Vakarelska-Popovska, M., Karadjova, V. & Velkov, Z. (2022). Synthesis, structure and prooxidant activity of 3-hydroxyflavone complexes with Cu(II). J. Chem. Technol. Metall. 57, 3.
40. Walencik, Paulina Katarzyna.,Choińska, R., Gołębiewska, E., & Kalinowska, M. (2024).Metal–Flavonoid Interactions-From Simple Complexes to Advanced Systems.Molecules, 29 (11), 2573.https://doi.org/10.3390/molecules29112573[2
41. Wenbin, Zhang., Duanbin, Li., Yu, Shan., Yecheng, Tao., Qinqinq, Chen., Tianli, Hu., Menghan, Gao., Zhezhe, Chen., Hangpan, Jiang., Changpin, Du., Win, Wang., Kai, Gua. (2023). Luteolin intake is negatively associated with all-cause and cardiac mortality among patients with type 2 diabetes mellitus.PMCID.
42. Weller, M. T., Overton, T., Rourke, J., & Armstrong, F. (2018). Inorganic Chemistry (2nd ed.). Oxford University Press.
43. West, A. R. (2017). Solid State Chemistry and Its Applications, 2nd ed. Wiley.
44. Yuanyong Yao., Meng Zeng., Laibing He., Yunyang Wang., and Shixue Chen (2020). Evaluation of General Synthesis Procedure for Bioflavonoids-Metal complexes in air-saturated alkane Solutions.Frontiers in Chemistry 8, 589.https//doi.org/10.fchm.2020.00589.